TRANSACTIONS ON ELECTROMAGNETIC SPECTRUM

Evaluation of Atmospheric Variability and Multipath Fade Statistics for Microwave Communication Applications over Akure, Nigeria

Ayodeji Gabriel Ashidi [1*], Victor Oyakhire Oviangbede [1*]

[1]Department of Physics, The Federal University of Technology, Akure, PMB 704, Akure, Nigeria

*** Corresponding author's e-mail address:** agashidi@futa.edu.ng

Received: 17 September 2025
Revised: 7 April 2026
Accepted: 22 April 2026

Research Article
Vol. 5 / No. 2 / 2026
Doi: 10.65819/tes.2026.v5i2.53

Abstract: The presence of multipath fading is one of the factors that contribute greatly to the performance of mm-Waves. This work considers the atmospheric factors and the multipath fade distribution over the region of Akure, Nigeria, using atmospheric measurements obtained through the Davis 6162 Vantage Pro2 weather station from January 2021 to December 2023. The geo-climatic factor and the fade depth exceedance probability distributions have been obtained for frequencies ranging from zero to 100 GHz with a path length of 5 km. The findings show a sudden increase in the fade depth when the frequency increases until about 16 GHz. Moreover, the effect of path length is quite noticeable on the amount of fade depth exceeded 0.01 percent of the time since there will be more fade depths when the path length increases due to several reflection effects owing to the bending effect of the radio wave from the refractivity gradient. It was found from this study that the month of January experienced the maximum outage probability rate with a geo-climatic factor of 1.81E-04, which can be considered ducting conditions. This suggests that there is a variation in atmospheric parameters like temperature, pressure, and moisture levels during different seasons and at different times of day, resulting in different fade depths.

Keywords: Multipath fading, Atmospheric variability, Communication systems, Fade depth exceedance, Microwave applications

Cite this paper as: Ashidi AG., Oviangbede VO., Evaluation of Atmospheric Variability and Multipath Fade Statistics for Microwave Communication Applications over Akure, Nigeria. Transactions on Electromagnetic Spectrum. 2026; 5(2): 25-34, Doi:10.65819/tes.2026.v5i2.53

1. INTRODUCTION

Communication using microwave technology, which lies in the frequency range from 1 GHz to 300 GHz, is one of the technologies that have made tremendous advances in recent times in the field of wireless communications, such as 5G and high-speed data communications [1]. There is increasing pressure in finding fast communication technology solutions, and hence the need for microwave technology in order to enable fast communication over short distances [2]. Nevertheless, the use of communication technology suffers from several challenges, especially when used in the tropics, since changes in the atmosphere have adverse effects on the microwave signal [3]. One of the problems faced in the transmission of microwave signals is multipath fading, in which case the signals travel along multiple paths to reach the destination [4].

© 2026 The Author(s). This work is licensed under CC BY-NC 4.0 | https://creativecommons.org/licenses/by-nc/4.0/

Multipath fading effects are even more severe in tropical areas such as Akure, Nigeria, owing to the intricate relationship between temperature, humidity, and pressure in these regions [4]. The accurate prediction and prevention of multipath fading are essential to improving the robustness and efficiency of microwave communications [5, 6]. This paper considers the variations in the atmosphere and multipath fading statistics in Akure, analyzing frequencies of up to 100 GHz. In this work, by considering in-situ atmospheric data, the role of various environmental factors in multipath fading effects is examined. Several studies have been conducted on the difficulties associated with multipath fading in microwave technology, specifically concerning high-frequency communication [7]. The sensitivity of the microwave signal to environmental factors like rain, humidity, and temperature fluctuations is well understood [8]. For example, [9] studied the effect of rain fading on line-of-sight microwave links, pointing out that this problem is particularly pronounced in tropical regions where there is abundant moisture and rainfall. Likewise, [10] looked into rain fade in Nigeria and showed how these environmental factors interfere with microwave communications. In addition to rain fading, multipath fading constitutes another major challenge in microwave communication technology. Kelmendi et al. [11] studied the problem of modeling propagation impairment and methods for mitigating fading for Earth-satellite communications. In their study, Kelmendi et al. considered the Ka-band, and the authors observed that multipath fading is a factor that could critically impact signal availability if appropriate measures are not taken. Several ways have been suggested for mitigating multipath fading in microwave systems. Some advanced methods such as beamforming and adaptive modulation were used for improving the quality of signals and avoiding interference. Furthermore, Muñoz et al. [12] carried out a detailed comparison of radiosonde meteorology data with the help of drones, satellite data, and WRF simulations. The experiment revealed the way in which UAVs can help collect real-time data about the atmosphere, thus enhancing the predictions related to the fading of signals. The results obtained through the use of UAVs show the significance of obtaining accurate information about the atmosphere in order to solve the problems related to fading in microwave communications. The present paper, however, takes into account previous studies and applies the knowledge gained from them to solving the problems of geo-climatic conditions and multipath fading statistics in Akure, Nigeria.

2. GEO CLIMATIC FACTOR AND FADE DEPTH

2.1. Geo-climatic Factor Determination

As noted in Section 1, the propagation of radio waves within the troposphere is affected by changes in climatic factors such as temperature, pressure, and humidity. These variables are linked to atmospheric refractivity, which can be represented by equation (1). In this expression, (N) denotes atmospheric refractivity, (n) is the refractive index of the atmosphere, (T) represents temperature (in Kelvin), (P) is the atmospheric pressure (in hPa), and (e) refers to the water vapor pressure (in hPa) [8].

$$N = (n-1)x10^6 = \frac{77.6}{T}(P + 4810\frac{e}{T}) \quad (1)$$

The water vapor pressure e is given by (2), where H (%) is the relative humidity and t (°C) is the air temperature:

$$e = \frac{6.1121H}{100}\exp(\frac{17.502t}{t+240.97}) \quad (2)$$

The refractivity gradient, which indicates how refractivity changes with altitude, is particularly important for line-of-sight (LOS) link designers. Multipath fading can occur only when this refractivity gradient in the atmosphere varies with height. The refractivity gradient is calculated using equation (3), where N_1 and N_2 represent the refractivity values at different altitudes, h_1 and h_2, respectively [8, 13]:

$$\frac{dN}{dh} \approx \frac{N_2 - N_1}{h_2 - h_1} \quad (3)$$

The frequency of occurrence of the refractivity gradient within the first 65 meters above ground level is evaluated. Following this, the cumulative distribution of the refractivity gradient (dN/dh) is calculated based on the observed frequency. The geo-climatic factor, which is useful for rapid planning, can be determined using the method outlined in ITU-R P539-12 (2015). In this process, (dN_1) represents the point refractivity

© 2026 The Author(s). This work is licensed under CC BY-NC 4.0 | https://creativecommons.org/licenses/by-nc/4.0/

gradient in the lowest 65 meters of the atmosphere, which is not exceeded for 1% of an average year, as specified by [14]:

$$K = 10^{-4.6-0.0027dN_1} \quad (4)$$

2.2. Fade Depth Prediction

The fade depth, in decibels (dB), is the ratio of the power of the reference signal to that of the faded signal [15]. ITU-R provides methods for determining the narrow-band fading distribution at deep fade depths, suitable for fast and detailed planning purposes. These approaches consist of three steps: first, determining the geo-climatic factor (K); second, calculating the path inclination; and finally, estimating the percentage of time that a specific fade depth (A) is exceeded during the worst month on average. Path inclination (εp) is derived using the heights of the transmitting and receiving antennas (he and hr), measured in meters above sea level, along with the path length (d) in kilometers [14].

$$|\varepsilon p| = |he - hr|/d \quad (5)$$

To get an approximate value for the third step for fast planning purposes, the equation (6) can be used, where pw is the percentage of time when fade depth A (dB) exceeds in the worst month on average, f is the frequency (GHz), hL is the height of the lower antenna (minimum of he and hr), d and K are distance and geo-climatic factor, respectively.

$$p_w = K\, d^{3.1}\,(1 + |\varepsilon p|)^{-1.29} f^{0.8} \times 10^{-0.00089h_L - A/10} \quad (6)$$

The continuous variation of the propagation medium results in the fact that the probability of obtaining a certain fade depth will be directly proportional to the probability of outage, and therefore to the availability probability of the link, provided that the specified fade depth results in the signal level being below the squelch threshold [16]. The proposed paper considers the application of the ITU-R method, which yields an average deviation of 5.9 dB from the actual value.

3. METHODOLOGY

3.1. Scope of Data and Study Location

The tropical location under consideration is Akure, Ondo State (as shown in Figure 1), situated in the Southwestern region of Nigeria. Positioned at latitude 7.15ºN and longitude 5.12ºE, Akure stands at an altitude of 358m. The tropical climate exhibits distinct wet and dry seasons, influenced by the south-west wind from the South Atlantic Ocean and the dry harmattan wind from the Sahara Desert. The region experiences temperatures ranging from 28°C to 31°C annually, with approximately 1,500 mm of rainfall and 80% humidity [4, 17]. The data set used in the present study is derived from the communication research group archive of the physics department, Federal University of Technology Akure (FUTA). They contain weather parameter values (temperature, pressure, humidity) measured within a three-year period, starting from January 2021 till December 2023, at the surface and 100 m altitude, using a Davis Vantage Vue weather station. Measures were taken to handle missing data. Data cleaning involved aggregation of recorded atmospheric parameters (taken each 30 minutes) into hourly, daily, and monthly averages. Further processing of the processed data was very helpful in explaining the refractivity gradient effect in tropical regions. Key atmospheric parameters such as temperature, pressure, and relative humidity underwent detailed examination, exploring diurnal and seasonal variations presented through graphs. Fade depth was estimated using the expression stated in equation (6). Other parameters, such as refractivity gradient and geo-climatic factor, were also estimated using equations (3) and (4), respectively, which aggregated to the formula used to estimate the fade depth. The formula presented in equation (6) above describes the ITU-R procedure in determining the percentage of time when a certain fade depth occurs. This procedure allows predictions to be made at fixed fade depth levels or at fixed percentages of outage. After determining the value of the geo-climatic factor, K, its values can be used in making predictions about the percentage of time a certain fade depth exceeds.

© 2026 The Author(s). This work is licensed under CC BY-NC 4.0 | https://creativecommons.org/licenses/by-nc/4.0/

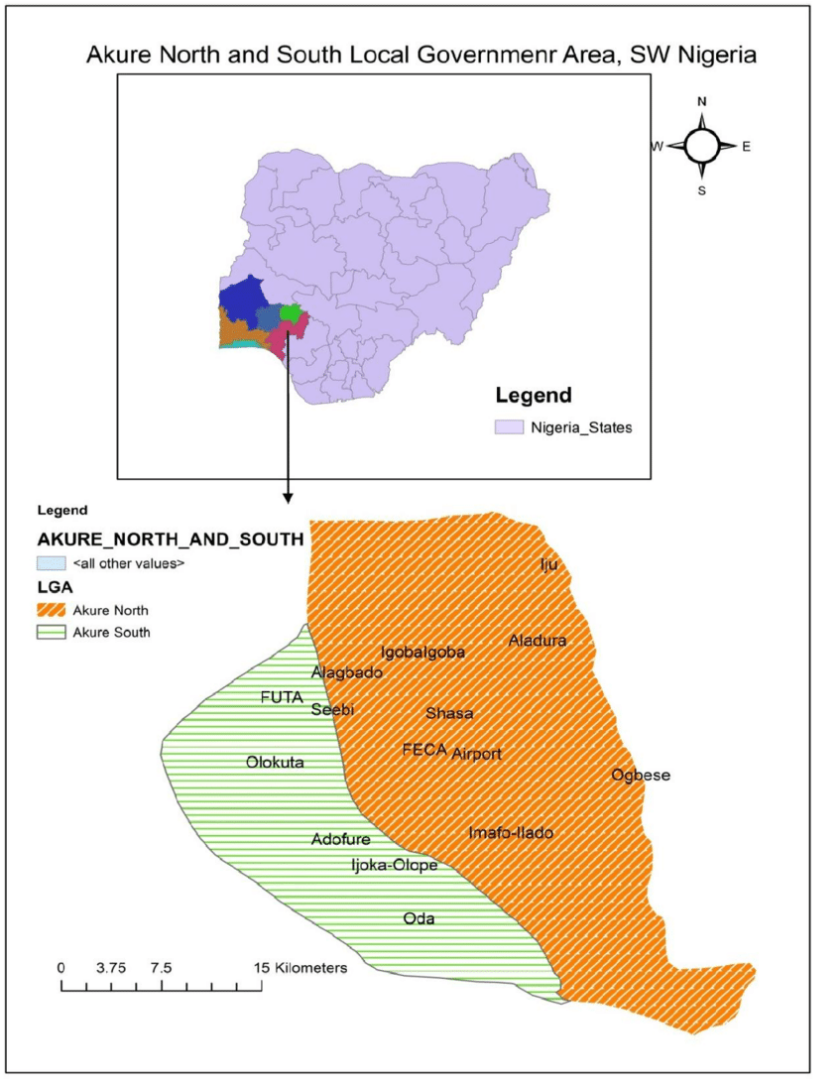

Figure 1. Map showing the study area showing key locations in Akure, Ondo State, Nigeria

4. RESULTS AND DISCUSSION

4.1. Variation of Atmospheric Parameters

Figure 2 (a) and (b) illustrate typical profiles of diurnal and seasonal variation of atmospheric temperature over Akure at two different altitudinal layers (surface level and 100 m) for the year 2022. Figure 2(a) reveals fluctuations in average temperature across different hours, with certain periods experiencing higher temperatures. Of particular interest is the fact that maximum and minimum temperatures are recorded at 15:00 hours (3:00 PM) and 06:00 hours (6:00 AM), respectively, both at surface and 100-meter levels. At both times, surface temperatures are higher than those at 100 meters, and the greatest temperature difference is seen at 15:00 hours (3:00 PM), whereas the least temperature difference is recorded at 06:00 hours (6:00 AM). This is explained by the Sun's impact on temperature, whereby surface temperatures increase during the day due to warming caused by sunlight and decrease at night as a result of cooling through radiation [9]. In addition, as can be seen from Figure 2(b), surface temperatures values are higher than those measured at 100 meters because of surface warming during the day and subsequent heat dissipation at night, resulting in higher surface layer temperatures [18]. Trends in temperatures are characterized by periodic wave changes with maximum temperatures in February and minimum temperatures in July, which is usual for tropical regions with stable seasonality changes [18, 19]. The location exhibits a consistently warm climatic characteristic with average monthly temperatures above 290 K (17°C) throughout the year, typical of equatorial regions. Temperature variations are relatively small, with a difference of about 5 K between the hottest and coldest months, a key characteristic of tropical climates. Meanwhile, nighttime temperature differences between ground and 100 meters levels are minimal, indicating limited ground heat release [6].

© 2026 The Author(s). This work is licensed under CC BY-NC 4.0 | https://creativecommons.org/licenses/by-nc/4.0/

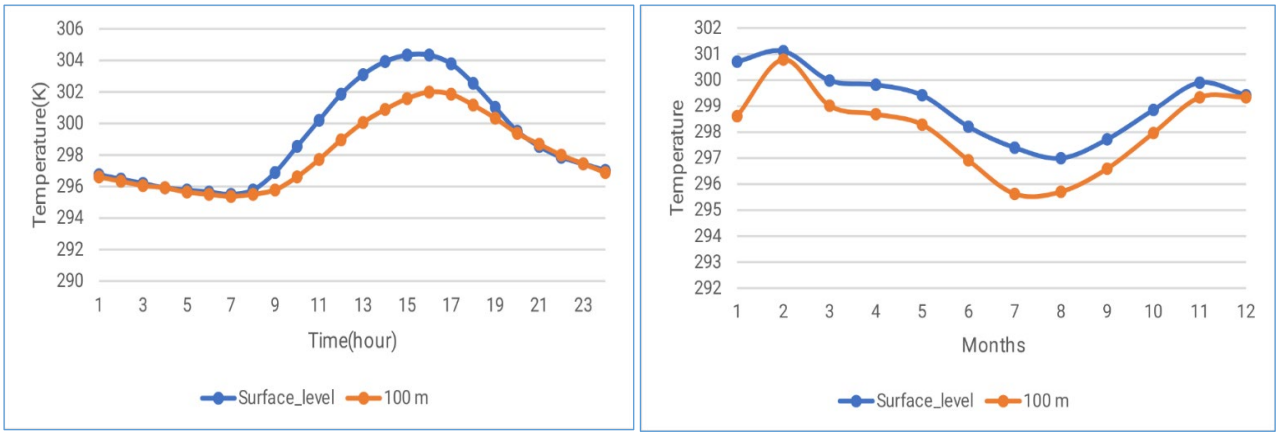

Figure 2. Typical profile of diurnal and seasonal variation of temperature at (a) the surface and (b) 100 m level

Similarly, Figure 3 (a) and (b) illustrates typical profiles of diurnal and seasonal atmospheric pressure variations at the surface and 100 m levels over Akure for the year 2022.

It is noted that the surface pressure consistently exceeds the pressure at 100 m altitude, which is attributed to the natural decrease of atmospheric pressure with increasing height. At both levels, the pressure exhibits a sinusoidal variation, with maxima occurring in the early morning and late afternoon and minima in the mid-morning and mid-afternoon, reflecting a typical diurnal cycle driven by solar heating [7]. The most significant pressure difference occurs between the morning, around 10 AM, and late afternoon, around 5 PM, from about 994 hPa to 990 hPa. Similar pattern is seen for the higher level with peak and least values of 991 hPa and 987 hPa respectively. Meanwhile, Figure 3(b), displays seasonal pressure variation profiles at ground and 100 m levels. Surface pressure values consistently exceed those at 100 meters throughout the year due to natural atmospheric pressure decrease with altitude. Both elevations follow a sinusoidal pattern, with pressure peaks around July and lows around January, opposing typical tropical temperature variation patterns [20], for both the surface and elevated layers.

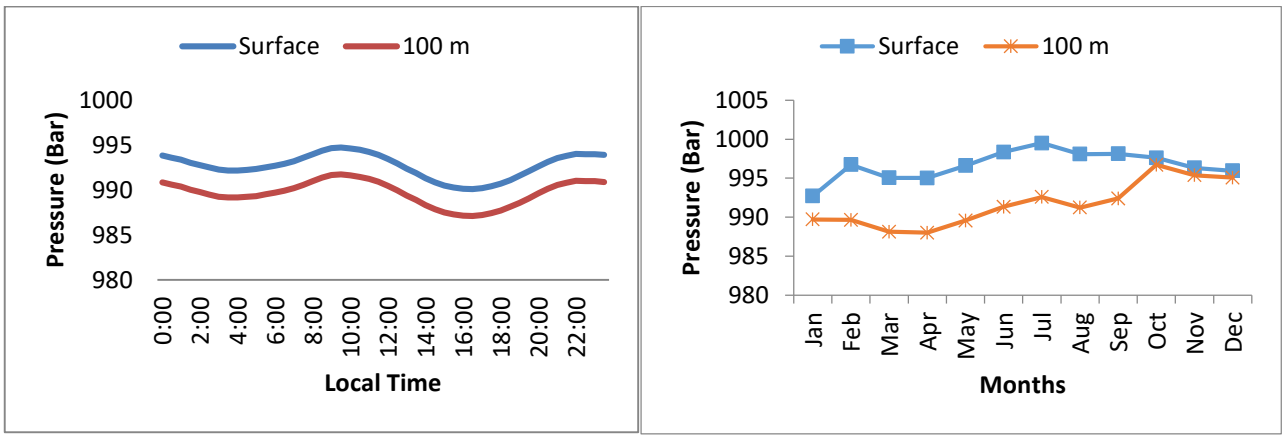

Figure 3. Typical profile of diurnal and seasonal variation of Pressure at (a) the surface and (b) 100 m level

Figure 4 (a), depicts the diurnal variation of humidity at surface level and 100m for the year 2022 respectively. Both elevations exhibit noticeable diurnal fluctuations in humidity, peaking in the early morning (around 6:00 AM - 7:00 AM) and dipping in the early afternoon (around 2:00 PM - 3:00 PM). Surface-level humidity consistently surpasses that at 100 meters throughout the day, with a margin ranging from about 10% to 15%. The most significant humidity difference between the two heights is spoted in the early morning and late evening (around 10% - 15%), diminishing to its smallest in the early afternoon (around 5% - 10%). This can be attributed to the effects of temperature differences. During night hours when there is cooling of the air, water vapor gets condensed resulting in low levels of humidity. With the sun rising and providing heat, evaporation occurs resulting in high levels of humidity, but then there is a fall as the temperature rises [20]. Additionally, the smaller humidity difference between the two heights at night is likely due to faster land cooling compared to higher altitudes, resulting in less temperature and evaporation contrast. Figure 4(b), illustrates the seasonal variation of humidity at surface level and 100m for the year 2023, depicting monthly changes in humidity. Both altitudes exhibit pronounced seasonal fluctuations in humidity, peaking during the wet season (April to October) and declining in the dry season (November to March). Surface-level humidity

© 2026 The Author(s). This work is licensed under CC BY-NC 4.0 | https://creativecommons.org/licenses/by-nc/4.0/

consistently surpasses that at 100 meters throughout the year, with a margin ranging from approximately 5% to 15%. The most substantial humidity difference between the two heights occurs in the wet season (around 10% - 15%), reducing to its smallest in the dry season (around 5% - 10%). The peak surface-level humidity reaches approximately 80%-85% in August, while the peak at 100 meters occurs around 75%-80% in July. Conversely, the lowest humidity at the surface level is around 45% in February, with the lowest at 100 meters at approximately 45% in February. The differences may be accounted for by the variations in temperature and precipitation levels, with the wet period showing higher precipitation levels and slightly lower temperatures, thus contributing to high evaporation and high humidity [21]. On the other hand, the dry period features low precipitation levels and higher temperatures, thus lower evaporation rates and humidity. Increased surface humidity levels can be explained by the availability of more water vapor at surface level. Moreover, the low difference in humidity levels in the dry season may be due to the rapid drying of the land surface relative to its elevation.

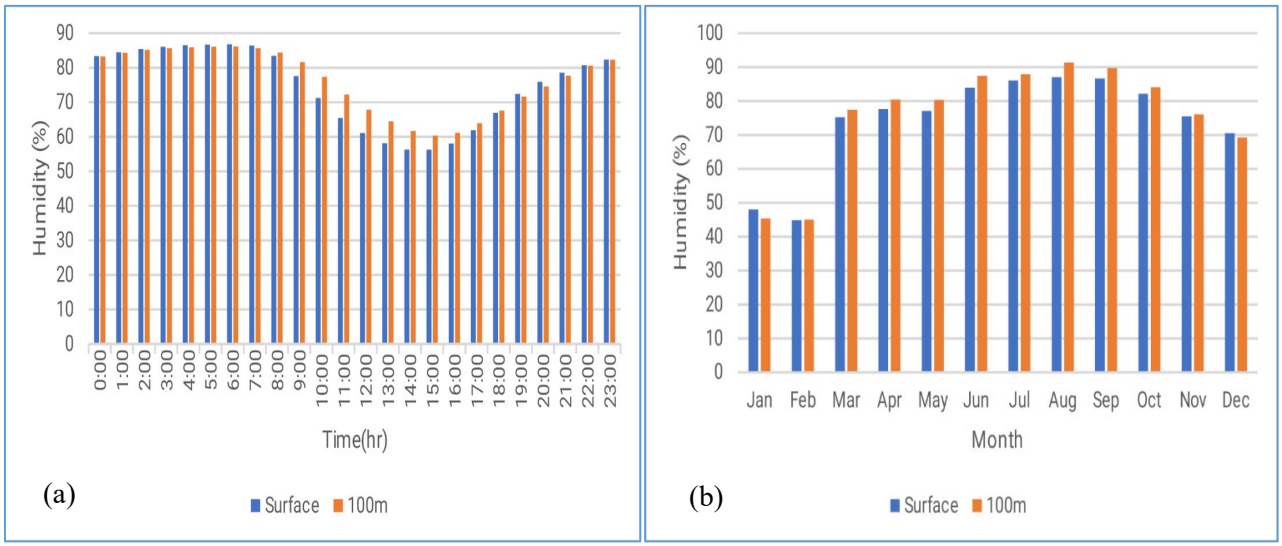

Figure 4. Typical profile of (a) diurnal and (b) seasonal variation of Humidity at the surface and 100 m level

4.2. Variation of Refractivity Gradient

In Figure 5(a), the chart shows the daily fluctuations of the refractivity gradient in a constant downward trend through the day. This starts at a value of -44 N-units/km at 3:00 AM and falls to its lowest level at 8:00 PM at a value of -98 N-units/km before rising slightly to approximately -70 N-units/km at 11:00 PM. There are instances where there are sharp falls at different times of the day like 1:00 AM to 2:00 AM and 5:00 PM to 6:00 PM, whereas there are also rises in value at certain periods, like 6:00 AM to 7:00 AM and 10:00 AM to 11:00 AM. Some of the determinants of this change include the temperature, pressure, and humidity, among others.

The graph in Figure 5(b) demonstrates the seasonal variation in the refractivity gradient, displaying a clear seasonal trend with maximums for the dry period (November to April) and minimums for the wet period (May to October). The maximum gradient value, which stands at around -25 N-units/km, is evident in January, whereas the minimum of about -45 N-units/km appears in August. During the course of months, there is an upward increase in gradient until April, with the maximum attained in January, while there is a downward decrease in gradient between May and August, where the lowest is attained in August. For the next two months (September to October), there is again an upward rise in the gradient but not as high as in the dry period. These fluctuations find explanations in temperature differentials, with the dry season's warmth resulting in a lower refractive index and thus a steeper negative gradient [22]. In contrast, the relatively cooler weather during the wet season results in a milder gradient. In addition to this, the humidity difference between the two seasons plays an important part, whereby the drier weather condition during the dry season creates the steeper gradient, whereas the wet season with its higher humidity levels creates a milder gradient to the earth surface. The little rainfall experienced during the dry season means low atmospheric aerosol content, which in turn affects the refractive index gradient. Other factors include geographical location and yearly differences among others that contribute to the formation of these characteristics [8].

© 2026 The Author(s). This work is licensed under CC BY-NC 4.0 | https://creativecommons.org/licenses/by-nc/4.0/

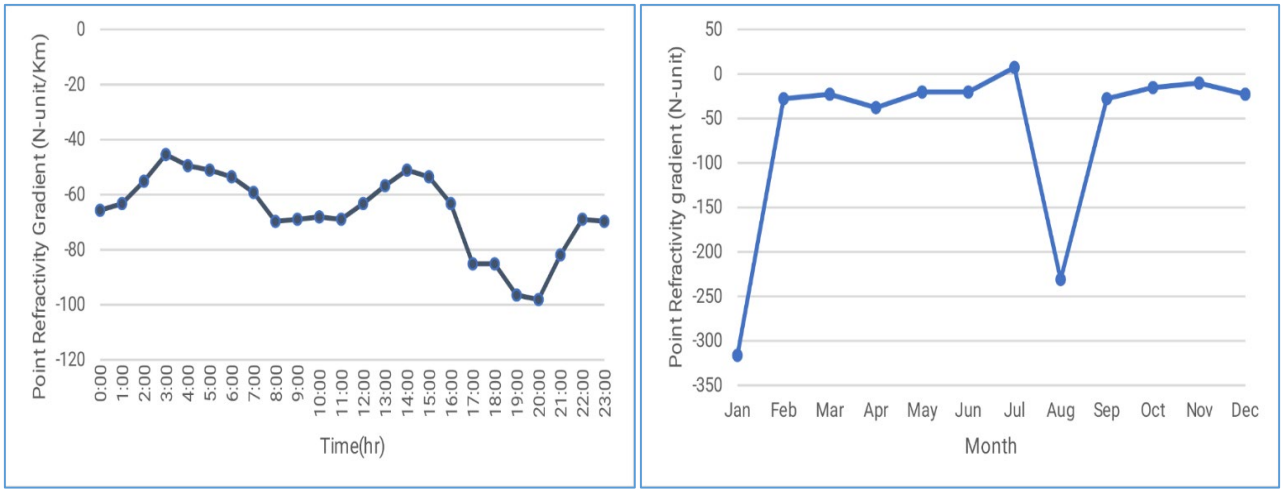

Figure 5. (a) Diurnal and (b) Seasonal variation of Refractivity gradient at the surface level and 100m for the year 2023

4.3. Variation of Geo-climatic Factor and Fade Depth

Figure 6 (a) is a depiction of the graph showing the yearly change in the Geo-climatic factor in the year 2022, which shows the changes occurring in this factor on a monthly basis. Since the Geo-climatic factor is directly associated with the point refractivity gradient function, it shows a similar trend but in reverse order. This Geo-climatic factor, represented by K, is one of the most critical elements in determining the outage probability of the worst month. An increase in Geo-climatic factors leads to fading of radio wave signals in a particular region. It was identified that there was the maximum outage probability in the month of January having the value of Geo-climatic factor K (1.81E-04). The Geo-climatic factor is indicative of path fade depth, suggesting that radio wave signals may encounter ducting conditions during such months [23]. Figure 6(b) shows the seasonal variations for the percentage of time when various fade depth values (5 dB, 10 dB, and 15 dB) are exceeded in Akure. In this case, it is apparent that the months of January and August always show relatively high percentages of time compared to the other months for all fade depths examined. Another interesting observation can be seen in the graph – there is an inverse relationship where the bigger the fade depth value, the lower the percentage of time when it was exceeded. The cause for this might have something to do with the atmospheric condition or weather experienced in those months. Another thing to consider is that, with a larger fade depth value, it is possible that such conditions only happen less frequently [24]. This may depend on seasons, for instance, atmospheric stability, temperature inversion, and other weather-related factors [25]. As illustrated in the figure, there is a rapid growth of fading depths with an increase in frequencies, especially around 16 GHz. Further, the rate at which the fading depth increases becomes less significant as the frequencies continue to grow. This data will be useful for determining the availability of systems in a particular period [9, 26].

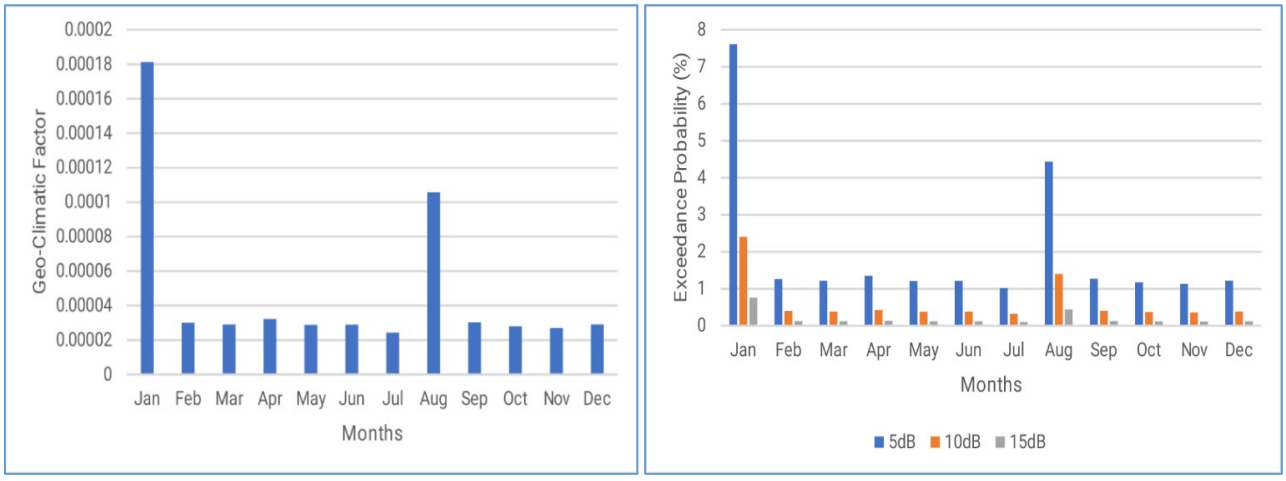

Figure 6. Seasonal variation of (a) Geo-climatic factor (b) percentage of time that different fade depth values (5dB, 10dB, and 15dB) are supposed in Akure

© 2026 The Author(s). This work is licensed under CC BY-NC 4.0 | https://creativecommons.org/licenses/by-nc/4.0/

In Figures 7(a-d), the percentage exceedance of the multipath fade for path length variation and frequencies over three years (2021, 2022, 2023), and the total period has been shown. From the graph, it can be seen that there is a great effect of the path length on the depth of fade exceeded. Longer path lengths exhibit higher values of fade depth exceedance, a phenomenon attributed to the increased prominence of the multipath phenomenon for extended distances [11]. This occurs due to multiple reflections caused by the bending of the radio beam induced by a more negative refractivity gradient [27]. This aligns well with the work of [28] which reported that "path attenuation remains notably low for shorter path differences while significantly increasing for longer ones, a relationship that underscores the direct correlation between path attenuation and path difference". Similarly, the observations also agree with the work of [29], which reported that "the free space path loss is highly dependent on the carrier frequencies", implying that "as the carrier frequency increases, the free space path loss will also increase". While it is a fact that other factors, such as the propagation environment and geometry, also contribute to fade depth variability, the role of increasing frequency cannot be overemphasized.

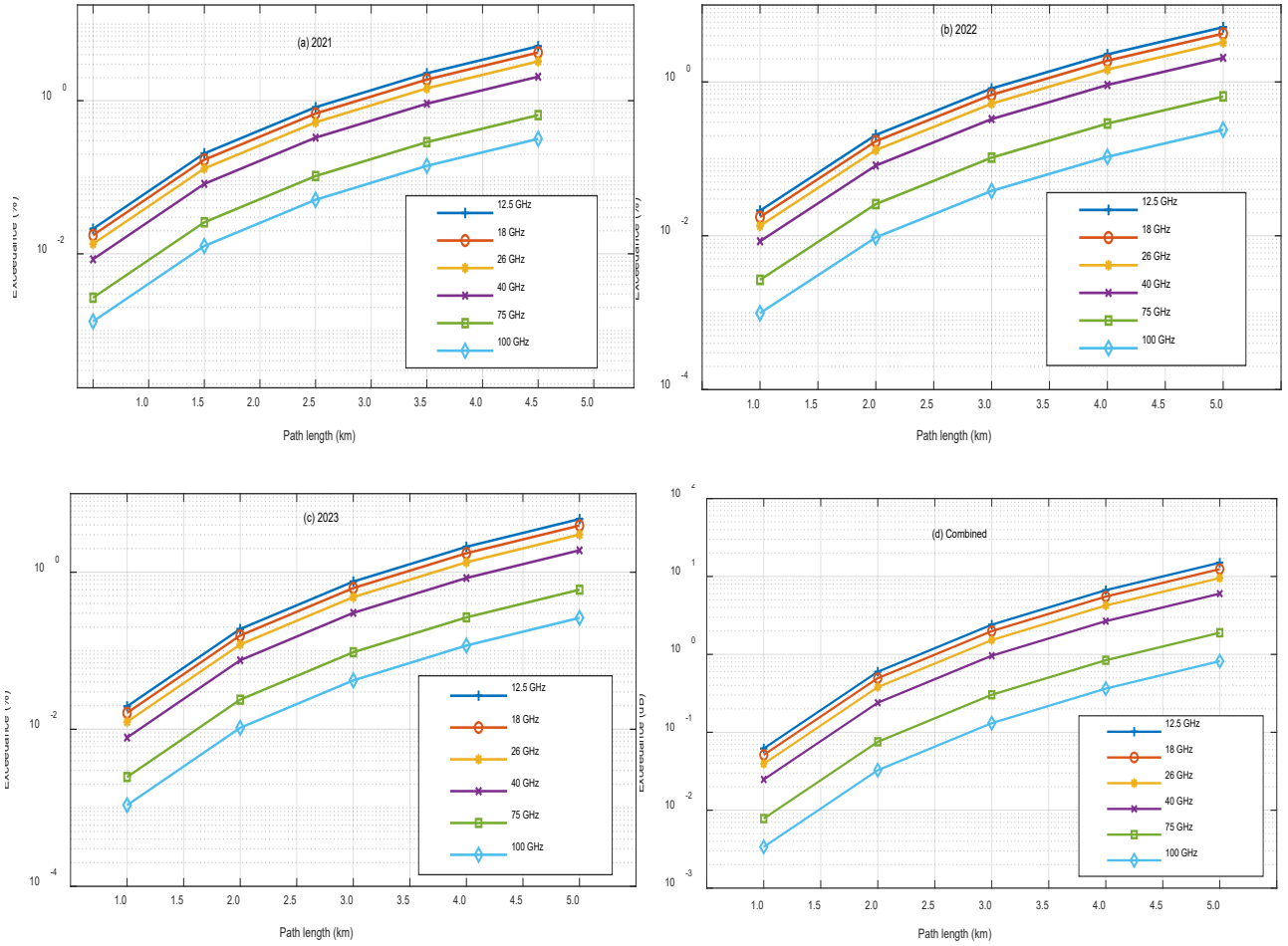

Figure 7. (a-d) Percentage exceedance of multipath fade with varying path lengths across different frequencies

5. CONCLUSION

The variation of the chosen primary radio-climatic parameters, i.e. atmospheric temperature, atmospheric pressure and atmospheric relative humidity, and secondary ones, such as refractivity gradient, geo-climatic factor, and multipath fade characteristics has been thoroughly examined throughout Akure, Nigeria. This analysis used meteorological data collected by the Davis 6162 Vantage Pro2 weather station between January 2021 and December 2023. The geo-climatic factor of the data and the probability of exceeding the fade depth at frequencies of 12.5, 18, 26, 40, 75, and 100 GHz over a 5 km terrestrial path were determined using these data. The findings indicate a steep rise in the depth of fading as frequency increases, especially to around 16 GHz after which the pace of fading level off. This is due to the fact that higher frequencies are becoming more sensitive to changes in the refractive index of the atmosphere and multipath interference effects. At the lower microwave frequencies, the wavelength is much larger than the inhomogeneities of the atmosphere, giving a

© 2026 The Author(s). This work is licensed under CC BY-NC 4.0 | https://creativecommons.org/licenses/by-nc/4.0/

smaller scattering and multipath effects. However, the higher the frequency, the shorter the wavelength, and thus the closer the wavelength is to the scale of refractive irregularities in the troposphere, the more the scattering, diffraction, constructive/destructive interference patterns that add to deeper fades.

The fact that the dependence on the path length on the fade depth is noticeable, also supports the importance of the atmospheric stratification and refractivity gradient. The more the propagation distance, the more there is a chance that a multi path will be formed as a result of reflections and refractions in layers of different refractive indices. Specifically, negative refractivity gradients (super-refraction) and steep temperature and humidity discontinuity gradients enhance ducting, where radio waves are trapped and guided in layers of the atmosphere, leading to ducting. This mechanism greatly increases the variability of the signal and adds to the increased fade depths, particularly at low time-percentage exceedances like 0.01%. The geo-climatic factor derived, with the maximum values obtained in January, represents the times of greater atmospheric instability and higher chances of aberrant propagation conditions. These are normally linked to high vertical gradients of temperature and moisture resulting in high refractivity gradients and multipath activity. These conditions falling into the ducting regime classification is congruent to the well-known theory of propagation where large values of the geo-climatic factor mean that the environment is susceptible to severe fading events. Moreover, the seasonal fluctuation in the statistics of fade shows the powerful effect of the local meteorology on the propagation of radio waves. Variations in atmospheric temperature

Acknowledgment

The authors express profound gratitude to the communications research group at the Federal University of Technology, Akure, for providing the data and an enabling environment for conducting this research.

Competing interests

The authors declare that there are no competing interests in this research work.

REFERENCES

[1] Ashidi A, Ojo J, Adediji A, Ajewole M. Characterization of Ku-band amplitude scintillation on earth-space path over Akure, SW Nigeria. XXXII General Assembly and Scientific Symposium, URSI; 2017.

[2] Ilori AO, Amusa KA, Erinosho TC. Digital terrestrial television in Nigeria: A technical review of path loss modeling and optimization techniques. International Journal of Advances in Applied Sciences. 2022;11(3):277. doi:10.11591/ijaas.v11.i3.pp277-286

[3] Alozie E, Abdulkarim A, Abdullahi I, Usman AD, Faruk N, Olayinka I-FY, et al. A Review on Rain Signal Attenuation Modeling, Analysis and Validation Techniques: Advances, Challenges and Future Direction. Sustainability. 2022;14(18):11744. doi:10.3390/su141811744

[4] Olalekan LO. Geo-spatial distribution of radio refractivity and the influence of fade depth on microwave propagation signals over Nigeria. International Journal of Physical Sciences. 2023;18(3):72-83. doi:10.5897/ijps2023.5036

[5] Ashidi AG, Dada JB, Lawal YB. Spectral Analysis of Ku-Band Scintillation Dataset for Satellite Communication in a Tropical Location. In: 2020 International Conference in Mathematics, Computer Engineering and Computer Science (ICMCECS); 2020/03. IEEE; 2020. p. 1-5. doi:10.1109/icmcecs47690.2020.240852

[6] Babarinde IO, Ojo JS, Ajewole MO. High-Capacity Millimeter Wave Channel for 5G and Future Generation Systems Deployment in Tropical Region using NYUSIM Algorithm. Transactions on Electromagnetic Spectrum. 2024;3(1):1-19. doi:10.5281/zenodo.8269340

[7] Sanyaolu ME, Ometan OO, Popoola FO, Owoyem SI, Soge AO, Willoughby AA. Radioclimatic Variable Characterization and Statistical Validation for Tropical Microwave Link Applications. Journal of Engineering Science and Technology Review. 2024;17(4):31-9. doi:10.25103/jestr.174.05

[8] Falodun SE, Ojo JS, Oviangbede VO. Spatial and Temporal Distribution of Modified Radio Refractivity Gradient at 875 hPa and 700 hPa over Nigeria. Physical Science International Journal. 2019:1-13. doi:10.9734/psij/2019/v23i330154

[9] Ogunsona DA, Ojo J, Ashidi A, Ajewole M. Characterization of rain fade dynamics for Ku band satellite communication systems in a tropical location. Journal of Physics: Conference Series; 2021. IOP Publishing. doi:10.1088/1742-6596/2034/1/012006

[10] Sodunke M, Ojo J, Adedayo K, De A, Sulaimon M. Prediction and analysis of seasonal rain attenuation in the South-western region of Nigeria for future microwave applications. Advances in Space Research. 2023;72(3):677-85. doi:10.1016/j.asr.2022.10.043

© 2026 The Author(s). This work is licensed under CC BY-NC 4.0 | https://creativecommons.org/licenses/by-nc/4.0/

[11] Kelmendi A, Švigelj A, Javornik T, Hrovat A. Propagation-Impairments Modelling and Fade-Mitigation Techniques for Earth-Satellite Links. Site Diversity in Satellite Communications: Modelling Using Copula Functions: Springer; 2023. p. 5-30. doi:10.1007/978-3-031-26274-6_2

[12] Muñoz LE, Campozano LV, Guevara DC, Parra R, Tonato D, Suntaxi A, et al. Comparison of Radiosonde Measurements of Meteorological Variables with Drone, Satellite Products, and WRF Simulations in the Tropical Andes: The Case of Quito, Ecuador. Atmosphere. 2023;14(2):264. doi:10.3390/atmos14020264

[13] Abu-Almal A, Al-Ansari K. Calculation of effective earth radius and point refractivity gradient in UAE. International Journal of Antennas and Propagation. 2010;2010(1):245070. doi:10.1155/2010/245070

[14] Series R. Propagation data and prediction methods required for the design of terrestrial line-of-sight systems. Recommendation ITU-R. 2015;530:12

[15] Asiyo MO, Afullo TJO. Statistical estimation of fade depth and outage probability due to multipath propagation in Southern Africa. Progress In Electromagnetics Research B. 2013;46:251-74. doi:10.2528/pierb12101212

[16] Ma X, Li Y, Li Z. The projection of canadian wind energy potential in future scenarios using a convection-permitting regional climate model. Energy Reports. 2022;8:7176-87. doi:10.2139/ssrn.3983074

[17] Ashidi AG, Ojo JS, Ajayi OJ, Akinmoladun TM. Evaluation of concurrent variation in rain specific attenuation and tropospheric amplitude scintillation over Akure, Southwest Nigeria. Earth Systems and Environment. 2021;5(3):547-59. doi:10.1007/s41748-021-00225-6

[18] Fei Y, Leigang S, Juanle W. Monthly variation and correlation analysis of global temperature and wind resources under climate change. Energy Conversion and Management. 2023;285:116992. doi:10.1016/j.enconman.2023.116992

[19] Ogunjo S, Adedayo K, Ashidi A, Oloniyo M. Investigating wind-solar hybrid power potential over Akure, southwestern Nigeria. J Niger Assoc Math Phys. 2013;23:511-6

[20] Adeyemi B, Ogodo S. Refractivity Gradient Variations and Intertropical Discontinuities Across Nigeria. International Astronomy and Astrophysics Research Journal. 2024;6(1):5-17

[21] Suleman KO, Suleiman SB, Sunmonu LA, SHEU AL. Estimation of refractivity gradients and effective earth radius factor (K-factor) in the lowest 100 m of the atmosphere over Ogbomoso, southwestern Nigeria. ITEGAM-JETIA. 2024;10(46):27-32. doi:10.5935/jetia.v10i46.1084

[22] Dekker M, Kazimierczuk AH, Garland RM, Stein-Zweers D, Levelt PF. Air quality in Africa from the telecoupled perspective: exploring interdisciplinary and transboundary scientific collaboration between Africa and the Global North. Global Sustainability. 2025;8:e34. doi:10.1017/sus.2025.10019

[23] de Medeiros FJ, de Oliveira CP, Avila-Diaz A. Evaluation of extreme precipitation climate indices and their projected changes for Brazil: From CMIP3 to CMIP6. Weather and Climate Extremes. 2022;38:100511. doi:10.1016/j.wace.2022.100511

[24] Legesse HE, Xiong L, Jingjing D. Rain Attenuation Prediction Modeling for Microwave and Millimeter Wave Band Using LSTM. 2024 4th International Conference on Machine Learning and Intelligent Systems Engineering (MLISE); 2024. IEEE. doi:10.1109/mlise62164.2024.10674324

[25] Misra A, Sarma MP, Sarma KK, Mastorakis N. Temporal deep learning assisted UAV communication channel model for application in EH-MIMO-NOMA set-up. Journal of Communications and Networks. 2022;24(2):166-83. doi:10.23919/jcn.2021.000045

[26] Nicolas Q, Boos WR. Understanding the spatiotemporal variability of tropical orographic rainfall using convective plume buoyancy. Journal of Climate. 2024;37(5):1737-57. doi:10.1175/jcli-d-23-0340.1

[27] Samad MA, Diba FD, Choi D-Y. A survey of rain fade models for earth–space telecommunication links—Taxonomy, methods, and comparative study. Remote sensing. 2021;13(10):1965. doi:10.3390/rs13101965

[28] Chuan LL, Roslee M, Sudhamani C, Waseem A, Osman AF, Jusoh MH. Path difference optimization of 5g millimeter wave communication networks in malaysia. Applied Sciences. 2023;13(19):10889. doi:10.3390/app131910889

[29] Nordin SF, Mansor Z, Ramli AF, Basarudin H. Propagation challenges in 5G millimeter wave implementation. Indonesian Journal of Electrical Engineering and Computer Science. 2019;15(1):274-82. doi:10.11591/ijeecs.v15.i1.pp274-282

© 2026 The Author(s). This work is licensed under CC BY-NC 4.0 | https://creativecommons.org/licenses/by-nc/4.0/